Thermochimica Acta 494 (2009) 35–39

Contents lists available at ScienceDirect

Thermochimica Acta

journal homepage: www.elsevier.com/locate/tca

Thermal analysis of ammonium trioxalatometallate complexes supported on titania and reducibility of their decomposition products

O.A. Kirichenko*, V.D. Nissenbaum, G.I. Kapustin, L.M. Kustov

N.D. Zelinsky Institute of Organic Chemistry, Russian Academy of Sciences, 47 Leninsky prosp., Moscow 119991, Russian Federation

ARTICLE INFO

Article history:
Received 9 February 2009
Received in revised form 15 April 2009
Accepted 17 April 2009
Available online 24 April 2009

Keywords:
Ammonium trioxalatometallate
TG-DTA
TPR

ABSTRACT

Thermal decomposition of the bulk and supported ammonium trioxalatometallate complexes $(NH_4)_3[M(C_2O_4)_3]\cdot xH_2O$, where M = Cr, Fe, Ru in air has been studied using TG-DTA, TPR, and XRD. The decomposition temperatures and behavior depend on the metal nature. The decomposition of the supported Cr complex occurs below 340 °C, whereas it lasts up to 380 °C for the bulk phase, and results in the formation of $CrO_{1.92}$ at 400 °C. First synthesized Ru trioxalato complex decomposed to $RuO_{1.8}$ in three stages before 315 °C, the decomposition being completed around 280 °C if the complex is supported on titania. Both bulk and supported Fe complex decomposed rapidly at the same temperatures to FeO_x with $x = 1.37$ for the supported system. The supported CrO_x and FeO_x phases are finely dispersed and X-ray amorphous. Their reduction with hydrogen below 500 °C resulted in Cr(III) and Fe(II) oxide species respectively. Only partial reduction to Fe^0 occurred at as high temperature as 850 °C. The $RuO_{1.8}/TiO_2$ system was reduced with hydrogen completely to Ru^0 below 300 °C.

1. Introduction

The transition metal oxalate complexes have found practical application as precursors of the nanocrystalline mono- and bimetallic oxides [1,2], catalysts [3], as well as the molecular magnetic materials [4,5]. The conditions of their thermal decomposition affect the material fabrication and properties required. Therefore, the thermal properties of the metal oxalate complexes have been extensively studied [6–15]. It has been found that the nature of the metal ions and gas media influence the decomposition of the anhydrous complexes. The oxalate complexes decomposed in air at the lower temperatures and in a different way [6,15] as compared with that in an inert atmosphere [13,14]. Unfortunately, there is still lack of publications on the thermal analysis of ammonium oxalatochromate complexes. Moreover, different chromium oxides were observed as the end products of trioxalatochromate decomposition. The Cr_3O_4 phase was formed during decomposition of $K_3Cr(C_2O_4)_3$ in an inert medium at 465–500 °C [13,14]. Thermal decomposition of chromium(III) trioxalatochromate [12] continued up to 670 °C in nitrogen, Cr_3O_4 formed being oxidized to Cr_2O_3 in air only at 860 °C. The same compound in air transforms to a mixture of Cr_3O_4 and Cr_2O_3 at around 460 °C. The decomposition of $(NH_4)_3[Cr(C_2O_4)_3]$ with variable morphology of crystallites (needles, polyhedra, platelets, spheres) at 350 °C in air leads to X-ray amorphous nonstoichiometric CrO_x, where x is close to 1.9 [10]. The crystallization of $CrO_{1.9}$ into α-Cr_2O_3 occurred on raising the temperature above 350 °C and was accompanied by the emission of oxygen in two steps.

The data presented above concern the decomposition of the bulk phases. Deposition of a precursor compound on a support matrix is required for the preparation of the supported oxide and metal nanoparticles. Supporting may effect the decomposition of the complexes. Preparation of the supported bimetallic phase is of high interest as well.

In the present paper, we examine the thermal decomposition of the ammonium trioxalatometallate complexes of trivalent Cr, Fe, and Ru, deposited on the titanium oxide support, as well as the reducibility of the decomposition products.

2. Experimental

The ammonium trioxalatometallate complex solutions were prepared as follows. The 0.48 M ammonium trioxalatochromate solution has been obtained according to the method proposed previously [16], which is based on the reaction

$$(NH_4)_2Cr_2O_7 + 7H_2C_2O_4 + 2(NH_4)_2C_2O_4$$
$$\rightarrow\ 2(NH_4)_3[Cr(C_2O_4)_3]\ +\ 6CO_2 + 7H_2O$$

The 0.73 M solution of ammonium trioxalatoferrate has been prepared by the procedure similar to that given in ref. [17] by mixing the ferric nitrate and ammonium oxalate solutions ($C_2O_4{}^{2-}$:Fe = 3:1) at

---

* Corresponding author. Tel.: +7 499 137 7073; fax: +7 499 137 2935.
E-mail address: okiriche@hotmail.com (O.A. Kirichenko).

0040-6031/$ – see front matter © 2009 Elsevier B.V. All rights reserved.
doi:10.1016/j.tca.2009.04.014

60 °C. Therefore, this solution contained ammonium nitrate as well. Preparation of $(NH_4)_3[Ru(C_2O_4)_3]$ was not described previously. We developed the novel procedure to synthesize this complex considering that the $C_2O_4{}^{2-}$ ion can easy substitute a CH_3COO^- ligand in $[Ru_2(\mu\text{-}O_2CCH_3)_4(H_2O)_2]^-$ species by mixing it with an equivalent amount of an aqueous solution of oxalic acid [18]. The chemical grade purity "Ru acetate trimer (Ru content 42.4 wt%)" (Strem Chemicals) was suspended into the oxalic acid solution ($H_2C_2O_4$:Ru = 3:1). The mixture was evaporated at 60 °C and treated with water several times until complete dissolution of the solid and absence of the acetic acid vapor. The ammonia solution was added to the final homogeneous solution in the molar ratio NH_3:Ru = 3:1. The dark green solution which is transparent in a thin layer or when diluted was obtained with the Ru content 0.063 mol l^{-1}.

The solid bulk phases of the ammonium trioxalatometallate complexes (designated as ATOFe, ATOCr, ATORu) were prepared by evaporation of the solutions at 60 °C. At higher temperatures dehydration of the crystallohydrates is possible [16]. Deposition of the complexes on the support was performed by immersing the support powder in an excess of the solution followed by evaporation under vigorous stirring and drying at 60 °C in air. The initial molar ratio of the support material and the material in solution was 14. The commercial TiO_2 aeroxide powder Degussa P 25 (70% anatase, 30% rutile, S = 50 m^2 g^{-1}, mean particle size 1.8 μm) was used as a support. As pHs of the solutions (3.0–3.5) are below point of zero charge of TiO_2 support (6.0) [19], the adsorption of anionic trioxalatometallate complexes occurs on the support surface in the suspension before precipitation. The adsorbed species are the centers for nucleation and particle growth of a dissolved compound, and precipitation proceeds predominantly on the support surface rather than in the bulk of solution [20]. The supported samples were designated as FeT, CrT, FeCrT, RuT. These samples were used for thermal analysis and for direct reduction in hydrogen flow at 400 °C. The samples for TPR studies were calcined preliminarily at temperatures, which were chosen based on the thermal analysis.

Thermal analysis was performed by the TG-DTA method using the Derivatograph-C instrument (MOM Company). The sample (about 0.02 g of the bulk phase or 0.05 g of the supported sample) was placed in a platinum crucible and heated in air from 20 to 400 or 600 °C at a heating rate 10 °C min^{-1}. Alumina was used as a reference in the DTA measurements. X-ray diffraction patterns were recorded in the range $2\theta = 10\text{–}60°$ using a DRON-2 diffractometer with Cu Kα radiation.

Temperature programmed reduction (TPR) measurements were performed in a laboratory constructed flow system built up from the gas purification and supply units, a quartz U-tube reactor, a water vapor trap and a thermal conductivity detector connected to a data acquisition unit. A water vapor trap was cooled to −100 °C. The detector was calibrated by the reduction of CuO (Aldrich-Chemie GmbH, 99%) pretreated in Ar flow at 300 °C. The sample (100 mg) was loaded in a reactor, and a thermocouple was mounted close to the sample. In order to minimize the contribution of adsorbed species to the TPR profiles, a sample was pretreated in argon at 80 °C for 1 h prior to the TPR experiment. The TPR run was carried out in a flow (30 ml min^{-1}) of the mixture of 4.6% H_2 in Ar at a heating rate of 10 °C min^{-1} in a temperature range of 30–850 °C.

3. Results

3.1. Thermal analysis

The thermogravimetric (TG) and corresponding derivative thermogravimetric (DTG) and differential thermoanalytical (DTA) curves of the samples prepared are shown in Figs. 1–4. The temperature ranges and the percentage mass losses are given in Tables 1 and 2.

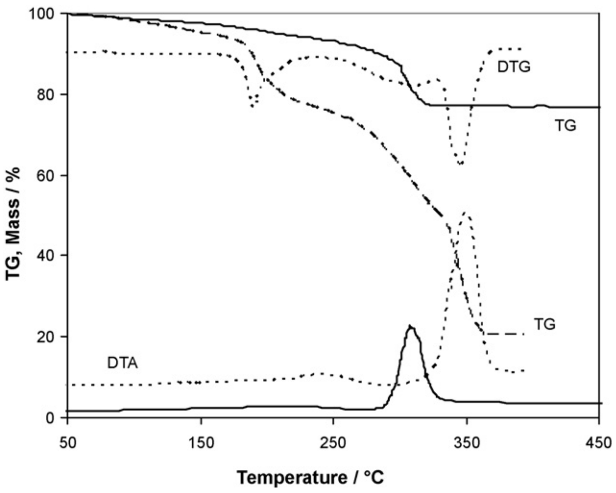

Fig. 1. TG, DTG and DTA curves of the supported and bulk (dashed lines) $(NH_4)_3Cr(C_2O_4)_3{\cdot}xH_2O$ phases.

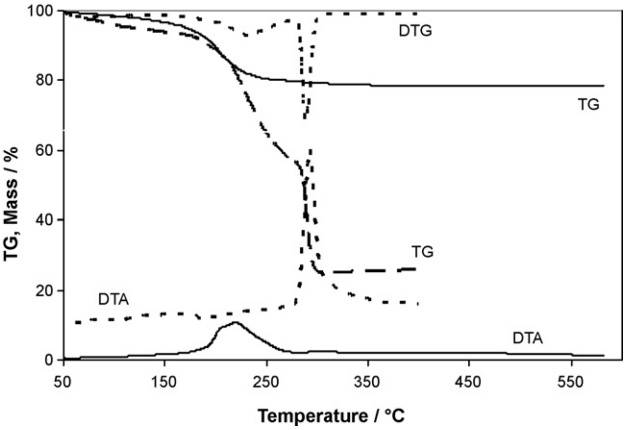

Fig. 2. TG, DTG, and DTA curves of the supported and bulk (dashed lines) $(NH_4)_3Ru(C_2O_4)_3{\cdot}xH_2O$ phases.

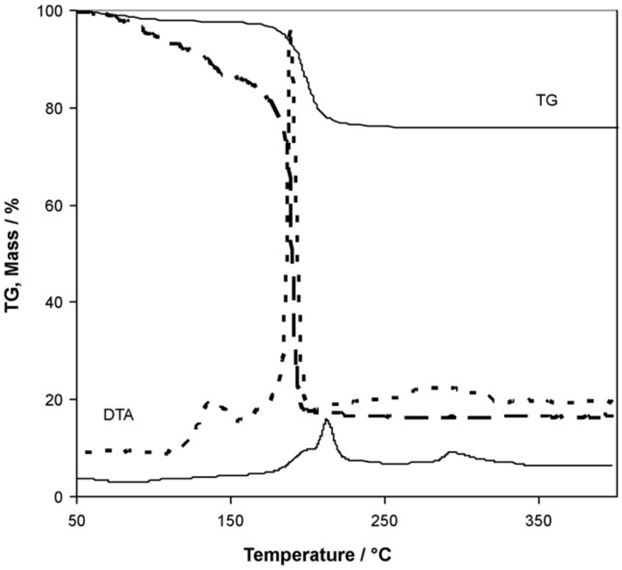

Fig. 3. TG and DTA curves of the supported and bulk (dashed lines) $(NH_4)_3Fe(C_2O_4)_3{\cdot}xH_2O$ phases.

Table 1
Temperature ranges and mass loss for the bulk ammonium oxalatometallates.

Sample ID	Temperature range on DTG; t_{max} (°C)	Δm (%)	Major heat effects; temperature ranges; t_{max} on DTA (°C)	Possible process	Δm_{calc} (%)
ATOCr	Up to 170	−5.9	$\Delta H > 0$	$-3H_2O$	−12.7
	170–245; 190	−17.4	$\Delta H < 0$, 200–245; 240	$-3NH_3$	−12.7
	245–330; 315	−26.3	$\Delta H > 0$; 290	$H_3Cr(C_2O_4)_3 \rightarrow Cr_2O_3$	
	330–380; 364	−30.1	$\Delta H < 0$, 305–385; 368		−56.8
	Total	−79.7		Total	−82.2
ATORu	Up to 170	−7	$\Delta H > 0$, 40–170	$-5H_2O$	−17.7
	174–283; 233	−35.7	$\Delta H > 0$, 175–240; 185	$(NH_4)_3Ru(C_2O_4)_3 \rightarrow Ru_2(C_2O_4)_3$	−36.5
	275–315; 296	−31.8	$\Delta H < 0$, 255–400, 305	$Ru_2(C_2O_4)_3 \rightarrow RuO_2$	−19.7
	Total	−74.5		Total	−73.9

Table 2
Temperature ranges and mass loss for the supported oxalatometallate phases.

Sample ID	Temperature range on DTG; t_{max} (°C)	Δm (%)	Major heat effects; temperature ranges; t_{max} on DTA (°C)	Possible process	Δm_{calc} (%)
FeT	35–120; 68	−2.8	$\Delta H > 0$, 40–95; 60	$-3H_2O$	−3.26
	150–250; 198	−21.4	$\Delta H < 0$, 150–245; 202	NH_4NO_3 decomposition; $(NH_4)_3Fe(C_2O_4)_3 \rightarrow Fe_3O_4$	−4.8; −17.8
		n/d	$\Delta H < 0$; 310	$Fe_3O_4 + O_2 \rightarrow Fe_2O_3$ or crystallization	+0.7
		n/d	$\Delta H < 0$; 344		
CrT	Up to 150	−2.6	$\Delta H > 0$	$-3H_2O$	−3.3
	150–225; 193	−3.4	–	$-3NH_3$	−3.3
	240–340; 314	−17.2	$\Delta H > 0$; 270 $\Delta H < 0$, 280–350; 320	$H_3Cr(C_2O_4)_3 \rightarrow Cr_2O_3$	−15.8
FeCrT	40–120; 95	−3.6	$\Delta H > 0$, 40–120; 85	$-3H_2O$	−4.0
	120–170; 158	−5.8	$\Delta H < 0$, 90–175; 155	NH_4NO_3 decomposition	−4.8
	170–220; 198	−17.7	$\Delta H < 0$; 215	$(NH_4)_3Fe(C_2O_4)_3 \rightarrow Fe_3O_4$	−17.8
	220–300; 230	−5.8	$\Delta H < 0$, 220–250; 230 $\Delta H < 0$, 250–300; 275		
RuT	Up to 120	−2.2	$\Delta H > 0$	$-H_2O$	–
	120–285; 208	−19.1	$\Delta H < 0$, 105–275; 227	$(NH_4)_3\ [Ru(C_2O_4)_3] \rightarrow RuO_2$	−18.7

The mass loss at temperatures 40–150 °C is in agreement with the data for the dehydration of the bulk $(NH_4)_3Fe(C_2O_4)_3{\cdot}3H_2O$ and $(NH_4)_3Cr(C_2O_4)_3{\cdot}3H_2O$ samples [13–16]. The obtained values of the mass loss due to dehydration are lower than the calculated values (Table 2) indicating partial dehydration of the supported compounds that were dried at 60 °C in an oven. Decomposition of the dehydrated complexes proceeds in several steps, as may be seen from the DTG and especially DTA curves, which contain several distinct maxima. The position of the most intensive DTG maximum varies with the central metal ion as follows:

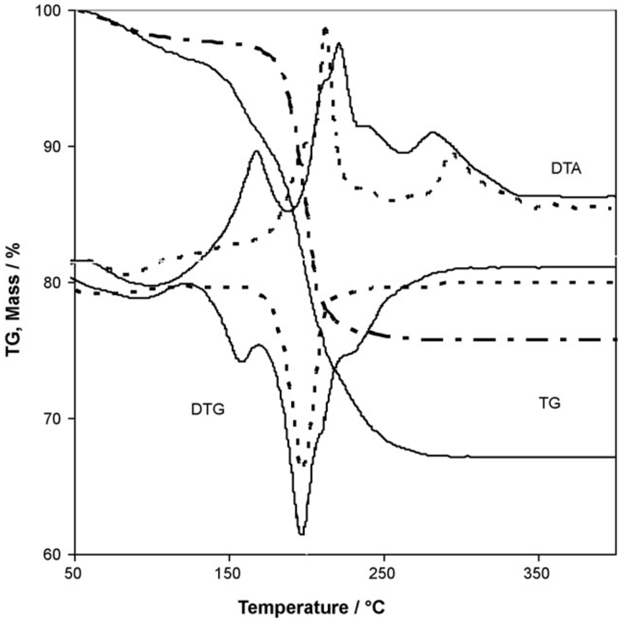

Fig. 4. TG, DTG and DTA curves of the FeCrT sample as compared with supported $(NH_4)_3Fe(C_2O_4)_3{\cdot}xH_2O$ (dashed lines).

Bulk phases:

Fe(204 °C) < Ru(296 °C) < Cr(364 °C)

Supported phases:

Fe(198 °C) < Ru(208 °C) < Cr(314 °C)

The ammonia trioxalatochromate decomposition is complex and proceeds in several steps (Fig. 1). The total mass loss is fairly close to the calculated one. The NH_3 elimination seems to occur before 245 °C, and then endothermic decomposition of trioxalatochromate ion starts. XRD patterns of the initial samples and after the TG-DTA run exhibited the reflections of the support only.

The sample ATORu, which was supposed to be ammonium trioxalatoruthenate crystallohydrate, is poorly crystalline. There are several weak reflections on its XRD pattern, the most intensive lines are at $2\theta = 28.70°$; 29.62°; 25.33°. The total mass loss for this sample is in agreement with the mass loss value calculated for the compound $(NH_4)_3[Ru(C_2O_4)_3]{\cdot}xH_2O$ with $x = 5$. The TG, DTG, and

DTA curves (Fig. 2) clearly indicate three stages of decomposition. The first one is a smooth release of water. The second one can be attributed to endothermic decomposition of an anhydrous complex to Ru(III) or Ru(II) oxalate. Comparison of TG data with calculated mass loss values (Table 1) gives a better fit for $Ru_2(C_2O_4)_3$. The third exothermic process may be the decomposition of oxalate with CO release and simultaneous exothermic oxidation of CO to CO_2 and Ru(III) to Ru(IV).

The decomposition curve of the sample with supported Ru complex (RuT) is smooth with no inflection up to 600 °C (Fig. 2). The main exothermic peak on the DTA curve is wide and looks like doublet with close intensities of the peaks at 210 and 225 °C. The XRD pattern of the initial sample exhibited the reflections of the TiO_2 support only. The changes in the shape and relative intensities of the reflections at $d/n = 3.25, 2.49, 1.70$, which appeared on the XRD pattern of the sample calcined at 400 °C for 2 h, can be attributed to the highly dispersed RuO_2 phase.

The TG curve of the supported $(NH_4)_3Fe(C_2O_4)_3$ sample is smooth with no inflection up to 250 °C (Fig. 3). Nevertheless, the DTA curve exhibits several exothermic peaks. The main exothermic peak is doublet with two close maxima at 190 and 202 °C. The similar double exothermic peak was observed earlier [6] during the decomposition of a bulk $(NH_4)_3Fe(C_2O_4)_3$ phase in air, but at higher temperatures of 250 and 255 °C. This difference in temperatures may be explained by the simultaneous exothermic decomposition of NH_4NO_3.

The XRD patterns of the initial samples and after the DTA-TG run exhibited the reflections of the TiO_2 support only. The residue obtained by evaporation of the solution at 60 °C was amorphous and its decomposition occurred in the same region as in the supported sample. The decrease in the temperature of decomposition for the supported sample may be explained by a smaller particle size of the $(NH_4)_3Fe(C_2O_4)_3$ crystallites on the support surface. Two weak exothermic peaks at 310 and 344 °C may be explained by oxidation of a residual amount of the Fe^0, FeO and Fe_3O_4 species the formation of which is possible in the lack of oxygen [13,15]. Another possible explanation is crystallization of the amorphous decomposition product. For comparison, XRD analysis of the product of the $(NH_4)_3Fe(C_2O_4)_3$ decomposition in air at 350 °C revealed both Fe_3O_4 and α-Fe_2O_3 phases [21]. Another research group [11] observed the formation of α-Fe_2O_3 only after calcination at 400 °C, whereas the samples calcined at 300 °C showed no XRD lines of any Fe oxide phase.

Introduction of $(NH_4)_3Cr(C_2O_4)_3$ into the ammonia trioxalatoferrate solution in the molar ratio 1:4 changed the decomposition behavior that can be clearly seen from the comparison of the TG, DTA and DTG curves (Fig. 4). There are no features of $(NH_4)_3Cr(C_2O_4)_3$ decomposition above 270 °C, but below this temperature at least three additional processes occurred indicating deposition of some mixed phases.

3.2. TPR

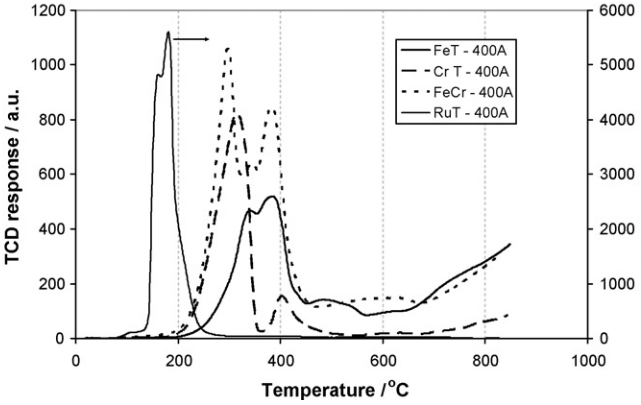

Fig. 5. TPR profiles of the samples calcined in air at 400 °C for 2 h.

Table 3
Hydrogen uptake on the MO_x/TiO_2 samples.

Sample ID[a]	Metal	ω (M) (wt%)	t (°C)	H_2 uptake ($mmol\ g^{-1}$)	H_2:M
RuT-400A	Ru	8.6	65–350	1530	1.80
CrT-400A	Cr	4.4	150–550	355	0.418
			150–360	313	0.368
			360–550	42	0.050
FeT-400A	Fe	4.8	150–580	314	0.365
			580–850		
FeT-400H	Fe	4.8	150–395	130	0.151
			395–580	186	0.216
			580–850		
FeCrT-400A	Fe (Cr)	4.8 (1.1)	100–325	314	(1.49)
			325–480	366	0.425
			480–680	150	0.175
			680–830	157	0.183
FeCrT -400H	Fe (Cr)	4.8 (1.1)	100–500	193	0.224
			500–850	353	0.410

[a] A—the samples calcined in air at 400 °C for 2 h; H—the samples after decomposition in hydrogen at 400 °C for 3 h and passivation with an air pulses at room temperature.

The TPR curve (Fig. 5) of the sample FeT-400A in the region 200–450 °C exhibited a double maximum of hydrogen consumption, the value of which (Table 3) is intermediate between that of $Fe_2O_3 \rightarrow FeO$ and $Fe_3O_4 \rightarrow FeO$ reduction. Therefore, the amorphous FeO_x phase includes both Fe^{3+} and Fe^{2+} ions. Smooth hydrogen consumption continued up to 850 °C, and reduction to Fe^0 was still uncompleted. One of the reasons of this reduction behavior may be the interaction of the FeO_x phase with the support. Also, the uncompleted two-step reduction $Fe_2O_3 \rightarrow Fe_3O_4 \rightarrow FeO$ at 330–700 °C was confirmed previously by TPR and XRD even for bulk highly dispersed phases [22]. In the same temperature region the higher hydrogen consumption in two steps was observed as well [23], and it was considered as a result of more complete reduction to Fe^0, also no data on the Fe content in the initial sample and its phase composition were presented.

The product of decomposition of the supported $(NH_4)_3Fe(C_2O_4)_3$ phase in hydrogen at 400 °C was easily reoxidized with air pulses at room temperature. TPR study of the reoxidized sample revealed broadness and shift to higher temperatures of the double peak (Fig. 6) with the same hydrogen consumption value below

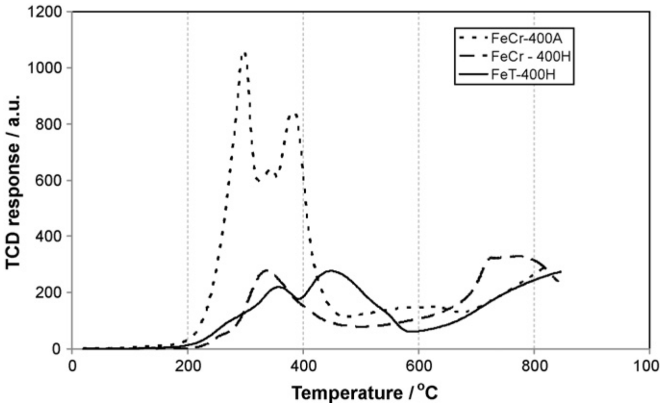

Fig. 6. TPR profiles of the samples after decomposition in hydrogen at 400 °C and passivation with air pulses at room temperature.

500 °C as for the calcined sample. It is known [24] that reduction of the bulk Fe-oxalate compounds in hydrogen results in the formation of Fe^0 species and complete reduction at temperatures above 360–380 °C. Reduction of the supported $(NH_4)_3Fe(C_2O_4)_3$ complex to Fe^0 may occur in our experiments as well, but metal particle size is too small to be stable in air at room temperature [25].

The intensive single maximum of hydrogen consumption followed by weak one was observed on the TPR curve (Fig. 5) of the sample CrT-400A. The possibility and extent of the reduction $Cr^{3+} \rightarrow Cr^{2+}$ are low. Only 1.6×10^{-7} mol Cr^{2+} per 1 mol of α-Cr_2O_3 were found in the sample reduced in hydrogen at 550 °C [26]. The H_2 amount required for this reduction is two orders of magnitude lower than the hydrogen consumption obtained in our TPR run. Two similar TPR peaks were observed earlier for the samples prepared by calcination of the chromium nitrate supported on titania [27,28], and they were attributed to reduction of Cr^{n+} ($n > 3$) to Cr^{3+} in polymeric chromate species (first peak) and in isolated chromate species (second peak). If we supposed similar reduction in the sample CrT-400A, the calculated oxide composition would be $CrO_{1.92}$ that is in good agreement with the results presented previously [10] for the products obtained from the crystalline trioxalatochromate phases after calcination in air at 350 °C. As the measured TG mass loss is even higher than that calculated for decomposition to Cr_2O_3, one can conclude that oxidation to $CrO_{1.92}$, which decreases the mass loss, proceeds under cooling of the sample in air after the TG-DTA run.

Reduction of the sample RuT-400A started above 100 °C and lasted up to 270 °C. The major hydrogen consumption occurred within the temperature range 140–200 °C. The hydrogen consumption value (Table 2) suggests the oxide composition of RuO_{2-x}, where $x = 0.2$.

The TPR curve of the calcined FeCrT-400A sample looks like superposition of the reduction curves of separate supported oxide products (Fig. 5), but the overall hydrogen uptake below 500 °C is almost twice as high as that calculated based on the data for FeT-400A and CrT-400A. Both the lower Cr loading as compared with CrT-400A and disordering of a mixed phase may be the reasons of the increased hydrogen consumption for FeCrT-400A. Previously [27] it was pointed out that the H_2:Cr ratio increased three times as CrO_x loading decreased from 5 to 1 wt%. Only one peak was observed below 500 °C on the reduction curve of the sample FeCrT-400H, exposed to air at room temperature (Fig. 6). The hydrogen consumption below 500 °C for this sample was only 28% of the value found for the calcined sample and 60% of the figure for FeT-400H. Comparison of TG-DTA and TPR results allows concluding that during preparation the ammonium trioxalatometallates formed some mixed phase whose decomposition in air or in hydrogen resulted in the species that included both Fe and Cr. There is some probability of $Fe_{3-x}Cr_xO_4$ formation in hydrogen at 400 °C.

4. Conclusions

Considering all information presented in this paper the following should be pointed out.

1. Thermal decomposition of the supported ammonium trioxalatometallate complexes $(NH_4)_3[M(C_2O_4)_3]\cdot xH_2O$, where M = Cr, Fe, Ru in air results in the formation of finely dispersed or X-ray amorphous nonstoichiometric oxide phases.
2. The temperature of decomposition of the supported complexes is lower than that of the bulk phases for Cr and Ru complexes.
3. The presence of ammonium nitrate decreases the decomposition temperature of the Fe complex phase. Both bulk and supported phases decomposed rapidly at the same temperature region which is below the decomposition temperature reported previously for the crystalline ammonium trioxalatoferrate.
4. The reduction of the supported CrO_x and FeO_x with hydrogen below 500 °C proceeds to Cr^{3+} or Fe^{2+}. Only partial reduction to Fe^0 occurred at temperatures as high as 850 °C.
5. The TPR and TG-DTA data allow one to suggest that the composition of the first synthesized water soluble complex compound of Ru with the oxalate ion may be close to $(NH_4)_3[Ru(C_2O_4)_3]\cdot 5H_2O$.
6. The RuO_x/TiO_2 system was reduced by hydrogen completely to Ru^0 below 300 °C.

Acknowledgement

Authors would like to express their gratitude to Professor I.V. Mishin for X-ray phase analysis of the samples and fruitful discussion of the results.

References

[1] D. Louër, A. Boultif, F.J. Gotor, J.M. Criado, Powder Diffr. 5 (1990) 162–164.
[2] T. Bataille, M. Louër, J.P. Auffredic, D. Louër, J. Solid State Chem. 150 (2000) 81–95.
[3] S.Yu. Taskina, O.A. Kirichenko, G.K. Chermashentseva, React. Kinet. Catal. Lett. 49 (2) (1993) 235–240.
[4] H. Tamaki, Z.J. Zhong, N. Matsumoto, S. Kida, M. Koikawa, N. Achiwa, Y. Hashimoto, H. Okawa, J. Am. Chem. Soc. 114 (1992) 6974–6979.
[5] S. Decurtins, H. Schmalle, R. Pellaux, New J. Chem. 22 (1998) 117–121.
[6] D. Broadbent, D. Dollimore, J. Dollimore, J. Chem. Soc. A (1967) 451–454.
[7] K. Nagase, Bull. Chem. Soc. Jpn. 46 (1973) 144–146.
[8] K. Nagase, K. Sato, N. Tanaka, Bull. Chem. Soc. Jpn. 48 (1975) 868–873.
[9] D. Dollimore, Thermochim. Acta 117 (1987) 331–363.
[10] A. Lerch, A. Rousset, Thermochim. Acta 232 (1994) 233–242.
[11] El-H.M. Diefallah, S.N. Basahel, A.A. El-Bellihi, Thermochim. Acta 290 (1996) 123–132.
[12] N. Deb, S.D. Baruah, N. Sen Sarma, N.N. Dass, Thermochim. Acta 320 (1998) 53–67.
[13] N. Rajić, D. Stojakovic, R. Gabrovšek, J. Therm. Anal. Calorimet. 63 (2000) 191–195.
[14] J. Li, F.-X. Zhang, Y.-W. Ren, Y.-Q. Hun, Y.-F. Nan, Thermochim. Acta 406 (2003) 77–87.
[15] M.A. Mohamed, A.K. Galwey, S.A. Halawy, Thermochim. Acta 429 (2005) 57–72.
[16] E.H. Merrachi, R. Cohen-Adad, F. Chassagneux, J. Paris, B.F. Mentzen, J. Bouix, Thermochim. Acta 152 (1989) 77–86.
[17] O.A. Kirichenko, V.A. Poluboyarov, Chem. Sust. Dev. 2 (1) (1994) 405–412.
[18] C.A. Murphy, T.S. Cameron, M.W. Cooke, M.A.S. Aquino, Inorg. Chim. Acta 305 (2000) 225–229.
[19] S. Tsubota, D.A.H. Cunninham, Y. Bando, M. Haruta, Stud. Surf. Sci. Catal. 91 (1995) 227–235.
[20] J.W. Geus, A.J. van Dillen, in: G. Ertl, H. Knozinger, J. Weitkamp (Eds.), Handbook of Heterogeneous Catalysis, vol. 1, Wiley, New York, 1998, pp. 240–257.
[21] O.A. Kirichenko, V.A. Ushakov, V.A. Poluboyarov, React. Kinet. Catal. Lett. 51 (1) (1993) 167–175.
[22] G. Neri, A.M. Visco, S. Galvagno, A. Donato, M. Panzalorto, Thermochim. Acta 329 (1999) 39–46.
[23] H.-Y. Lin, Y.-W. Chen, C. Lil, Thermochim. Acta 400 (2003) 61–67.
[24] V. Carles, P. Alphonse, P. Tailhades, A. Rousset, Thermochim. Acta 334 (1999) 107–113.
[25] Y.-P. Sun, X.-Q. Li, J. Cao, W.-X. Zhang, H.P. Wang, Adv. Colloid. Int. Sci. 120 (2006) 47–56.
[26] K.I. Slovetskaya, F.N. Aiginin, A.M. Rubinshtein, Izv. AN SSSR. S. Chim. 9 (1972) 1969–1973 (in Russian).
[27] S.D. Yim, I.-S. Nam, J. Catal. 221 (2004) 601–611.
[28] U. Scharf, H. Schneider, A. Baiker, A. Wokaun, J. Catal. 145 (1994) 464–478.